The Heparan Sulfate Proteoglycan Syndecan Is an In Vivo Ligand for the *Drosophila* LAR Receptor Tyrosine Phosphatase

A. Nicole Fox and Kai Zinn

Supplemental Experimental Procedures

Screening for LAR Ligands

The extracellular domain of LAR (aa 33–1377) fused to a C-terminal PLAP sequence was cloned into a baculovirus expression vector, pVL1393 (BD Biosciences) [S1, S2]. The LAR signal sequence (aa 1–32) was replaced with the gp67 signal sequence. Baculoviruses were generated and used to infect Sf9 cells, and supernatant media were collected at the appropriate time after infection, as evaluated by measuring fusion protein levels. The fusion proteins were quantified by measuring AP activity as described previously [S3]. Conditioned media, containing secreted LAR-AP fusion protein, was incubated with live-dissected embryos. If strong staining was not observed, we concentrated the media 5–10× with an Amicon concentrator. This usually increased staining efficacy; however, we found that some batches of medium did not stain well even if concentrated. In these cases, we generated more medium from a new infection. These protocols were used in the same manner to generate fusion proteins for DPTP10D, DPTP99A, DPTP69D, DPTP4E, LAR-HS1-AP, LAR-HS2-AP, and others.

To detect binding, stage 16 embryos were manually dechorionated, transferred to an agar block, and lined up, ventral side up and anterior at the top. The line of embryos was transferred onto a strip of double-stick tape attached to a SuperFrostPlus glass slide within a rectangle of wax (about 30 × 20 mm) laid down by a PAP pen. The embryos (now dorsal side up) were immediately flooded with 1× phosphate-buffered saline (PBS: 1 mM KH_2PO_4, 155 mM NaCl, 3 mM Na_2HPO_4-$7H_2O$ [pH 7.4]). They were then removed from the vitelline membrane by cutting through it with a glass needle, transferred onto the glass, and dissected to create a filet. Most of the PBS was removed, and then 200 μl of undiluted LAR-AP fusion protein supernatant was added with a P1000 at the same time as the remaining PBS was removed from the opposite corner of the well with another P1000. Fusion protein aliquots were centrifuged for 10 min at maximum speed at 4°C before addition. This replacement of the PBS by supernatant was done so as to minimize dilution of the supernatant as much as possible without exposing the embryos to air. The embryos were incubated for 1–2 hr at room temperature in a moisturized chamber. LAR-AP was then exchanged for 5% formaldehyde in 1× PBS without prewashing (fix was added simultaneously with removal of the supernatant as described above for the PBS/supernatant exchange, then the slides were washed 3× more with larger volumes of fix). The embryos were fixed for 45 min to 1.5 hr at room temperature. The fix was then exchanged for 1× PBS (3 washes of ~2 ml each) and then for PBT (1× PBS, 1 mg/ml BSA, 0.05% Triton-X100; 3 more washes). Embryos were blocked in PBT with 5% normal goat serum (PBT+NGS) for 10–30 min at room temperature. Embryos were incubated with 200 μl rabbit anti-PLAP in PBT + NGS (from Biomeda in the experiments described here, and used at 1:600; however, new lots of the Biomeda antibody are made against a different antigen [recombinant rather than placental] and do not work well. In recent experiments we have employed an anti-PLAP rabbit antibody from Serotec at 1:500) overnight at 4°C. The embryo slide was washed in a tray with PBT (3 washes; >1 hr total), reblocked, and incubated with goat-anti-rabbit Alexa488 (Molecular Probes; 1:1000 in PBT + NGS). Secondary and tertiary antibodies from 1:10 stocks were preabsorbed in PBT on wild-type fixed embryos to reduce background, then stored at 4°C with NaN_3 to prevent bacterial growth. The slides were washed again, visualized to make sure the staining had worked, then washed with PBS and cleared with 70% glycerol for >1 hr. Most of the glycerol was removed after clearing and a coverslip installed. Compound microscope images were obtained with an Olympus camera and Magnafire software.

For the deficiency screen, we first balanced the entire Df kit over GFP balancers. We dissected >4 nongreen embryos and >2 green (GFP-balancer) embryos (*Df*/+) in each slide well. The same lines were simultaneously screened with DPTP69D-AP, so that staining with each RPTP-AP provided a control for the other and also indicated whether the line in question formed embryos with enough structure to allow visualization of staining. mAb BP102 can also be added at 1:10–1:20 to the secondary antibody to allow simultaneous visualization of the axon ladder; BP102 staining is then visualized with an antimouse fluorescent secondary antibody.

Table S1. Genotypes Tested for LAR-AP Staining

	LAR-AP Fusion Protein Staining	
	CNS Axons	Muscle Attachment Sites
Key Df Crosses		
Df(2R)C4 × Df(2R)*Egfr5*	+	+
Df(2R)AA21 × Df(2R)*Egfr5*	+	—
Mutants		
Sdc^{Df48}	+	—
Sdc^{10608}	+	—
Sdc^{KG06163}	+	—
Sdc^{Df48}, Ubi-*Sara*/*Sdc*^{10608} × *Sdc*^{Df48} (maternal/zygotic mutant)	+	—
Sara^{250}	+	+
Fkbp13^{M34}	+	+
dally^{06464}	+	+
dally^{80}*dlp*^{A187}	+	+
trol^{13}	+	+
sgl^{A31}	+	—
sfl^{03844}	+	—
ttv^{00681b}	+	—
pipe^{1}	+	+
lar$^{13.2}$/*lar*$^{5.5}$	+	+
Other Binding Experiments (Wild-Type Embryos)		
LAR-AP + heparin	+	—
EphA3-AP	—	—
PLAP	—	—
LAR-AP + excess PLAP	—	—
LAR-HS1-AP	+	—
LAR-HS2-AP	+	—

Plus sign indicates normal LAR-AP staining. Minus sign indicates absent LAR-AP staining, in either the CNS or muscle attachment sites. Most of these entries are discussed in the text. Note that *Egfr* deficiencies can only be screened in crosses to proximal deficiencies such as *Df(2R)AA21*, because removal of *Egfr* prevents CNS development. Thus, *Df(2R)Egfr5*, which is part of the deficiency kit and removes *Sdc*, could not be screened directly. The table also shows that LAR-AP normally to *pipe* mutants. Pipe is a putative 2-O-sulfotransferase that is implicated in production of specific sulfated GAG isoforms; this indicates that the particular modification that Pipe performs is not necessary for LAR-Sdc interactions.

Supplemental References

S1. Flanagan, J.G., and Cheng, H.J. (2000). Alkaline phosphatase fusion proteins for molecular characterization and cloning of receptors and their ligands. Methods Enzymol. *327*, 198–210.

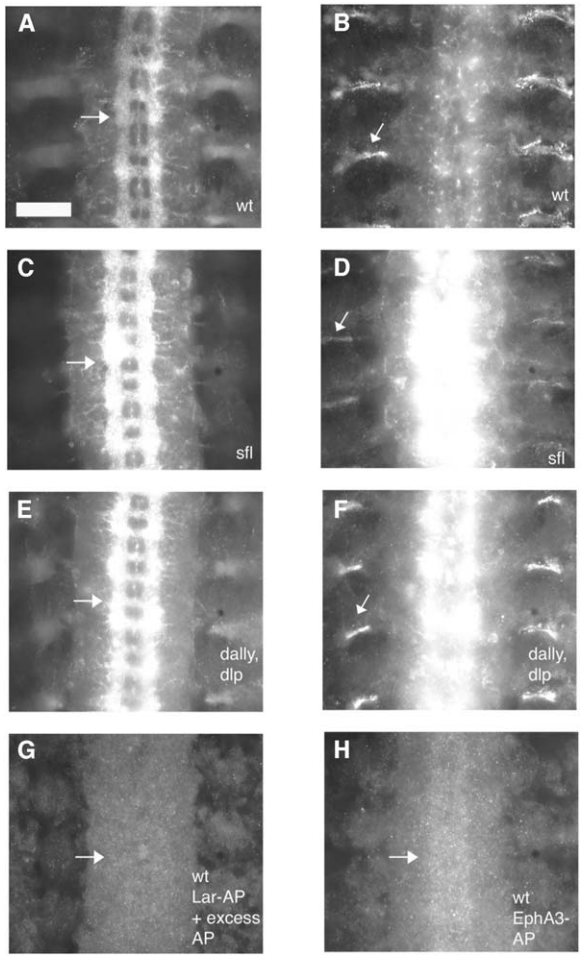

Figure S1. LAR-AP Binding to *sfl* and *dally dlp* Embryos, and Binding Controls

(A) Wild-type (wt) embryo, middle focal plane, showing LAR-AP staining of CNS axons (arrow).

(B) Wild-type embryo, ventral focal plane, showing LAR-AP staining of muscle attachment sites (arrows).

(C) sfl^{03844} (zygotic *sfl* mutant) embryo, middle focal plane, showing LAR-AP staining of CNS axons (arrow).

(D) *sfl* embryo, ventral focal plane. LAR-AP stains the muscle attachment sites to a much lesser extent than with wild-type embryos (compare to [B]). The dot-like staining pattern is missing, while some residual lines of staining remain (arrow), much as in *Sdc* embryos (Figure 1E).

(E) $dally^{80}$, dlp^{A187} embryo (zygotic *dally dlp* mutant), middle focal plane, showing LAR-AP staining of CNS axons (arrow).

(F) *dally, dlp* ventral focal plane, showing LAR-AP staining of muscle attachment sites (arrow). This LAR-AP staining is indistinguishable from wt embryos (compare to [B]).

(G) Wild-type embryo incubated with LAR-AP, followed by anti-PLAP antibody preincubated with excess commercial PLAP. No signal is detected on the CNS axons (arrow) or at muscle attachment sites. This experiment demonstrates that the staining pattern observed is dependent on the presence of the human AP epitope on the embryo via binding of LAR-AP, rather than to cross-reaction of the secondary or tertiary antibody with a *Drosophila* epitope.

(H) Wild-type embryo incubated with EphA3-AP (gift of J. Flanagan). Faint staining in a midline strip is observed (arrow). This pattern does not resemble the LAR-AP staining pattern.

Scale bar is approximately 10 μm. All images were taken with 40× objective and 1.25× ocular at the same exposure settings for comparison purposes.

S2. Flanagan, J.G., Cheng, H.J., Feldheim, D.A., Hattori, M., Lu, Q., and Vanderhaeghen, P. (2000). Alkaline phosphatase fusions of ligands or receptors as in situ probes for staining of cells, tissues, and embryos. In Applications of Chimeric Genes and Hybrid Proteins Pt. B, Volume *327*, QA (QA: QA), pp. 19–35.

S3. Cullen, B.R., and Malim, M.H. (1992). Secreted placental alkaline phosphatase as a eukaryotic reporter gene. Methods Enzymol. *216*, 362–368.

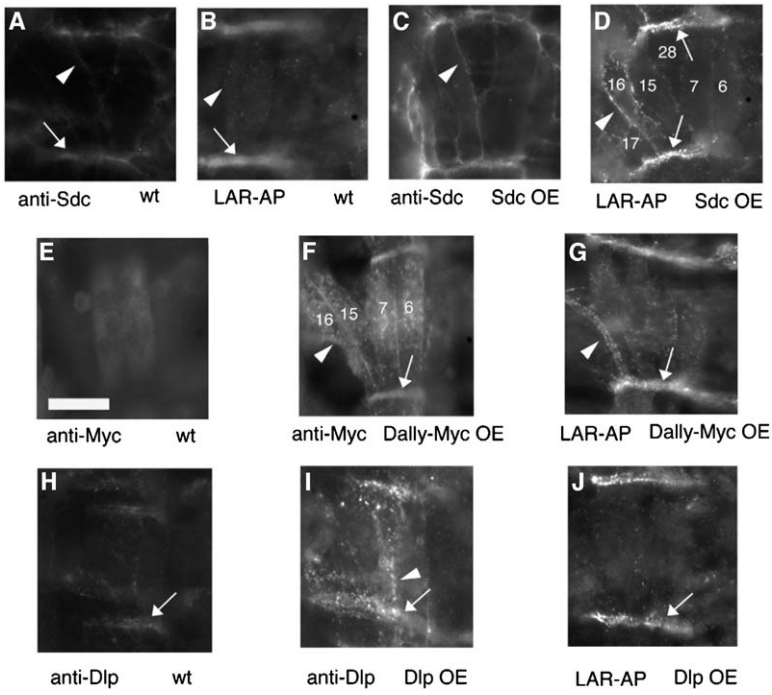

Figure S2. LAR-AP Binds to Ectopically Expressed Sdc and Dally Proteins

All images show the ventral muscles spanning an abdominal hemisegment on the right side of a live-dissected stage 16 embryo filet. Anterior is up. Staining is visualized by immunofluorescence (40× objective). Muscle morphologies look somewhat different with these stains than when muscles are visualized by DIC optics. The muscles that are prominent in these images are labeled in (D) and (F). See http://www.its.caltech.edu/~zinnlab/motoraxons/muscle%20diagrams.html for a schematic diagram of muscles. Arrows indicate muscle attachment sites. Arrowheads indicate muscle fiber edges. Scale bar equals 10 μm.

(A) Anti-Sdc staining, wild-type muscles.

(B) LAR-AP staining, wild-type muscles. Muscle attachment sites (out of focus) stain but not the muscles.

(C) Anti-Sdc staining of muscles of 24B-GAL4 (muscle driver) × UAS-Sdc embryos (Sdc overexpression).

(D) LAR-AP staining of muscles of 24B-GAL4 × UAS-Sdc embryos. LAR-AP now stains muscle edges. Note the dot-like character of the staining.

(E) Anti-Myc staining of muscles of a UAS-Dally-Myc control embryo with no driver.

(F) Anti-Myc staining of muscles of a 24B-GAL4 × UAS-Dally-Myc embryo (Dally-Myc overexpression). Dally-Myc is now expressed at high levels on the muscles.

(G) LAR-AP staining of muscles of a 24B-GAL4 × UAS-Dally-Myc embryo. Note bright dot-like staining of muscles.

(H) Anti-Dlp staining of muscles of a UAS-Dlp control embryo with no driver. Weak staining is observed at the muscle attachment sites.

(I) Anti-Dlp staining of muscles of a 24B-GAL4 × UAS-Dlp embryo (Dlp OE). Dlp is now expressed at high levels in the muscles.

(J) LAR-AP staining of muscles of a 24B-GAL4 × UAS-Dlp embryo. Note the lack of bright muscle staining; muscle attachment sites stain normally. The fact that LAR-AP does not brightly stain Dlp on muscles could indicate that embryonic Dlp lacks some enzymatic modification required for LAR binding. Alternatively, perhaps the levels of ectopic Dlp attained in our experiments were insufficient to bind enough LAR-AP for visualization.

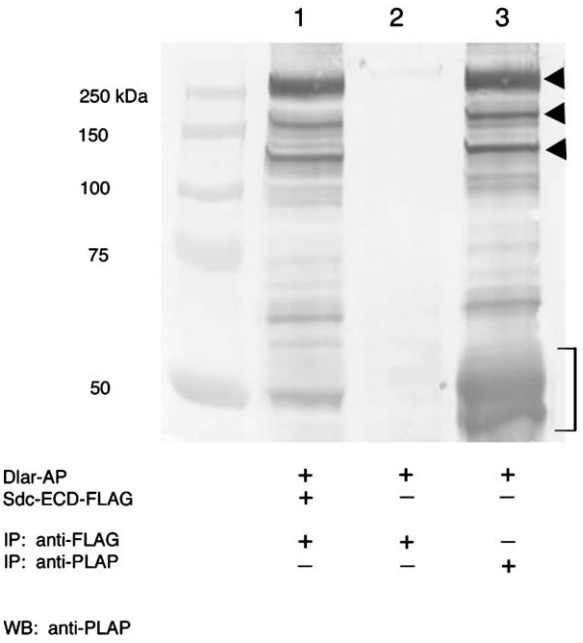

Figure S3. Coimmunoprecipitation of LAR-AP and Sdc

Lane 1: LAR-AP and Sdc-ECD-FLAG (from 293T cells) were incubated together and immunoprecipitated by anti-FLAG mAb. Lane 2: LAR-AP alone immunoprecipitated with anti-FLAG, showing no cross-reaction of LAR-AP with anti-FLAG. Lane 3: LAR-AP immunoprecipitated with anti-PLAP, showing the amount of LAR-AP input and the sizes of the LAR-AP bands. After gel electrophoresis and transfer, the blot was probed with anti-PLAP. There are three main species of LAR-AP that are commonly visualized (arrowheads), the largest of which is ~260 kDa; all three precipitate with Sdc-FLAG. Note the large amount of material at the bottom of lane 3 (bracket); this is LAR-AP that has been cleaved near the LAR/PLAP junction, and the PLAP portion is detected on the blot. As expected, this material does not precipitate with Sdc-FLAG (compare with lane 1).

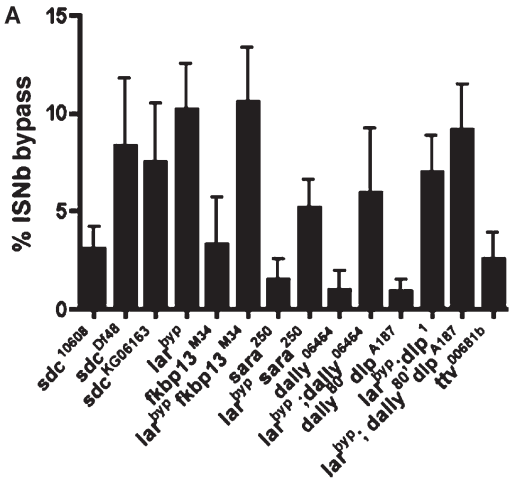

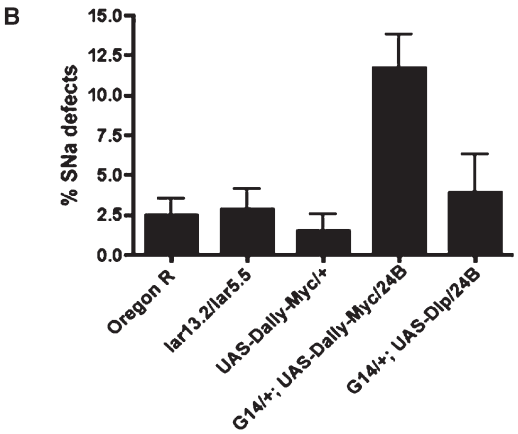

Figure S4. Additional Genotypes from Genetic Interaction Experiment and Epistasis Experiment

(A) Bar graph showing ISNb bypass phenotypic percentages in different mutant combinations. Number of abdominal hemisegments (A2–A7) scored are as follows: Sdc^{10608} = 257; Sdc^{Df48} = 239; $Sdc^{KG06163}$ = 191; Lar^{bypass} = 211 (also in Figure 5); $Fkbp13^{M34}$ = 125; Lar^{bypass}, $Fkbp13^{M34}$ = 125; $Sara^{250}$ = 132; Lar^{bypass}, $Sara^{250}$ = 233; $dally^{06464}$ = 195; Lar^{bypass}; $dally^{06464}$ = 83; $dally^{80}$, dlp^{A187} = 230; Lar^{bypass}; dlp^{1} = 156; Lar^{bypass}; $dally^{80}dlp^{A187}$ = 111; ttv^{00681b} = 107. This figure shows that the zygotic *Sdc* mutants do not display ISNb bypass at a high penetrance (<8%) and that *Sara*, *Fkbp13*, *dally*, and *dlp* mutations do not exhibit genetic interactions with Lar, because the penetrance of the bypass phenotype in all these combinations is not greater than that seen for Lar^{bypass} alone (~10%).

(B) Bar graph showing penetrance of SNa phenotypes in various genetic backgrounds. All SNas with at least one missing or obviously truncated branch were scored as mutant. These results show that muscle overexpression of Dally produces SNa phenotypes at a low penetrance (~11%, versus 18% for Sdc overexpression; Figure 7); Dlp overexpression does not produce phenotypes. Number of abdominal hemisegments (A2–A7) scored are as follows: *Oregon R* = 226; $Lar^{5.5}/Lar^{13.2}$ = 138; UAS-Dally-Myc/+ = 108; G14/+; UAS-Dally-Myc/24B = 154; G14/+; UAS-Dlp/24B = 99. G14 and 24B are muscle GAL4 drivers; elav is a panneuronal driver.

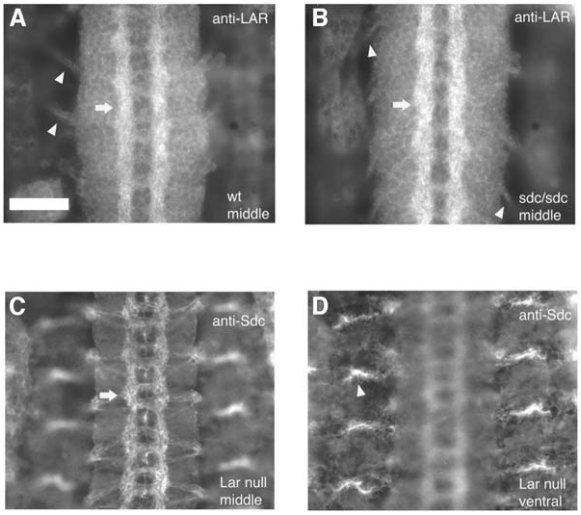

Figure S5. LAR and Sdc Localization Are Unchanged in *Sdc*/*Sdc* Maternal/Zygotic Mutants and $Lar^{5.5}/Lar^{13.2}$ Embryos, Respectively

This experiment demonstrates that the removal of LAR does not cause a redistribution of Sdc, and vice versa. If a substantial amount of the Sdc visualized in embryos were cleaved, shed material, and bound to LAR, one might have expected that Sdc localization would change in a *Lar* mutant; this is not observed. This figure also shows LAR localization on CNS axons.

(A) Wild-type (wt) embryo stained with anti-LAR in the absence of detergent, middle focal plane. Anti-LAR labels the CNS (arrow) and motor nerves exiting the CNS (arrowheads). The staining of motor nerves, which only contain a few axons, is very faint, because LAR is a rare protein. Thus, we could not directly visualize LAR together with Sdc on motor axons in the periphery. Therefore, in Figure 5 we used anti-HRP as a marker to visualize the position of the nerves relative to the patches of Sdc expression.

(B) Sdc^{Df48},*ubi-Sara*/$Sdc^{10608} \times Sdc^{Df48}$ (maternal/zygotic mutant; see text for description) stained with anti-LAR, middle focal plane. The expression pattern is indistinguishable from that seen in wild-type embryos.

(C and D) $Lar^{5.5}/Lar^{13.2}$ embryo stained with anti-Sdc, middle focal plane (C) and ventral focal plane (D). The expression pattern is indistinguishable from wild-type embryos (compare to Figures 1F and 1G). In the absence of LAR, Sdc is still expressed on the CNS (arrow [C]) and muscle attachment sites (arrowhead [D]).

Scale bar is approximately 10 μm. Images were taken with 40× objective and 1.25× ocular.